INTERNATIONAL JOURNAL OF MARITIME TECHNOLOGY

IJMT Vol.5/ Winter 2016 (27-39)

Available online at: http://ijmt.ir/browse.php?a_code=A-10-296-4&sid=1&slc_lang=en

Stress Concentration Factors in Uniplanar Tubular KT-Joints of Jacket Structures Subjected to In-Plane Bending Loads

Hamid Ahmadi[1*], Ali Ziyaei Nejad[2]

[1] *Assistant Professor, Faculty of Civil Engineering, University of Tabriz; h-ahmadi@tabrizu.ac.ir*
[2] *MSc Student, Faculty of Civil Engineering, University of Tabriz; aliziaee89@gmail.com*

ARTICLE INFO

Article History:
Received: 10 Jan. 2016
Accepted: 15 Mar. 2016

Keywords:
Fatigue
Offshore jacket structure
Tubular KT-joint
Stress concentration factor (SCF)
In-plane bending (IPB)

ABSTRACT

In the present research, data extracted from the stress analysis of 46 finite element models, verified using test results obtained from an experimental investigation, were used to study the effect of geometrical parameters on the chord-side stress concentration factors (SCFs) of central and outer braces in uniplanar tubular KT-joints of offshore structures subjected to four different types of in-plane bending (IPB) loads. Parametric study was followed by a set of the nonlinear regression analyses to develop SCF parametric equations for the fatigue analysis and design of uniplanar tubular KT-joints under IPB loadings.

1. Introduction

The main structural components of jacket-type platforms, commonly used for the production of oil and gas in offshore fields, are fabricated from circular hollow section (CHS) members by welding the prepared end of brace members onto the undisturbed surface of the chord, resulting in what is called a tubular joint (Figure 1a).

Tubular joints are subjected to cyclic loads induced by sea waves and hence they are susceptible to fatigue damage due to the formation and propagation of cracks. Significant stress concentrations at the vicinity of the welds are highly detrimental to the fatigue life of a tubular connection. For the design purposes, a parameter called the stress concentration factor (SCF) is used to quantify the stress concentration. This calls for greater emphasis in accurate calculation of the SCFs to estimate the fatigue life of offshore structures.

The SCF, defined as the ratio of the local surface stress at the brace/chord intersection to the nominal stress in the brace, exhibits considerable scatter depending on the joint geometry, loading type, weld size and type, and the considered position for the SCF calculation around the weld profile. Under any specific loading condition, the SCF value along the weld toe of a tubular joint is mainly determined by the joint geometry. To study the behavior of tubular joints and to easily relate this behavior to the geometrical characteristics of the joint, a set of dimensionless geometrical parameters has been defined. Figure 1b depicts a simple uniplanar tubular KT-joint with the geometrical parameters τ, γ, β, ζ, α, and α_B for chord and brace diameters D and d, and their corresponding wall thicknesses T and t. Critical positions along the weld toe of the brace/chord intersection for the calculation of SCFs in a tubular joint, i.e. saddle, crown, toe and heel, have been shown in Figure 1c.

There is a rich literature available on the study of SCFs in tubular joints:

- For unstiffened uni-planar joints, the reader is referred for example to Kuang et al. [1], Wordsworth and Smedley [2], Wordsworth [3], Efthymiou and Durkin [4], Efthymiou [5], Hellier et al. [6], Smedley and Fisher [7], UK HSE OTH 354 [8], and Karamanos et al. [9] (for the SCF calculation at the saddle and crown positions of simple uni-planar T-, Y-, X-, K-, and KT-joints); Gho and Gao [10], Gao [11], and Gao et al. [12] (for the SCF determination in uni-planar overlapped tubular joints); and Morgan and Lee [13, 14], Chang and Dover [15, 16], Shao [17, 18], Shao et al. [19], Lotfollahi-Yaghin and Ahmadi [20], and Ahmadi et al. [21] (for the study of the SCF distribution along the weld toe of various uni-planar joints).
- For unstiffened multi-planar joints, the reader is referred to Karamanos et al. [22] and Chiew et al. [23] (for the SCF calculation in XX-joints); Wingerde et al. [24] (for the SCF determination in KK-joints); Karamanos et al. [25] (for the study of SCFs in DT-joints); and Lotfollahi-Yaghin and Ahmadi [26], Ahmadi et al. [27, 28] and Ahmadi and Lotfollahi-Yaghin [29] (for the comprehensive investigation of SCFs in two- and three-planar tubular KT-joints), among others.

- For various types of stiffened joints, the reader is referred to Dharmavasan and Aaghaakouchak [30], Aaghaakouchak and Dharmavasan [31], Ramachandra et al. [32], Nwosu et al. [33], Ramachandra et al. [34], Hoon et al. [35], Myers et al. [36], Woghiren and Brennan [37], and Ahmadi et al. [38, 39], Ahmadi and Lotfollahi-Yaghin [40], and Ahmadi and Zavvar [41], among others.
- For other SCF-related studies such as probabilistic and reliability analyses, the reader is referred for example to Ahmadi et al. [42], Ahmadi and Lotfollahi-Yaghin [43, 44], Dallyn et al. [45], and Ahmadi et al. [46, 47].

In the present paper, results of numerical investigations of the stress concentration in uniplanar tubular KT-joints are presented and discussed. In this research program, a set of parametric finite element (FE) stress analyses was carried out on 46 steel tubular KT-joints subjected to four different types of IPB loading (Figure 2). Depending on the wave incident angle, location of the joint, relative position of the wave crest, and design load combination, these types of IPB loading can actually occur. The analysis results were used to present general remarks on the effect of geometrical parameters including τ (brace-to-chord thickness ratio), γ (chord wall slenderness ratio), β (brace-to-chord diameter ratio), and θ (outer brace inclination angle) on the SCFs at the crown, toe, and heel positions. The saddle position was not studied. The reason is that under the IPB loadings, the nominal stress at this position is zero and hence the determination of SCFs is not needed. Based on the results of KT-joint FE models, verified using experimental measurements, a SCF database was prepared. Then, a new set of SCF parametric equations was established, based on nonlinear regression analyses, for the fatigue analysis and design of uniplanar KT-joints subjected to IPB loadings. The reliability of proposed equations was evaluated according to the acceptance criteria recommended by the UK DoE [48].

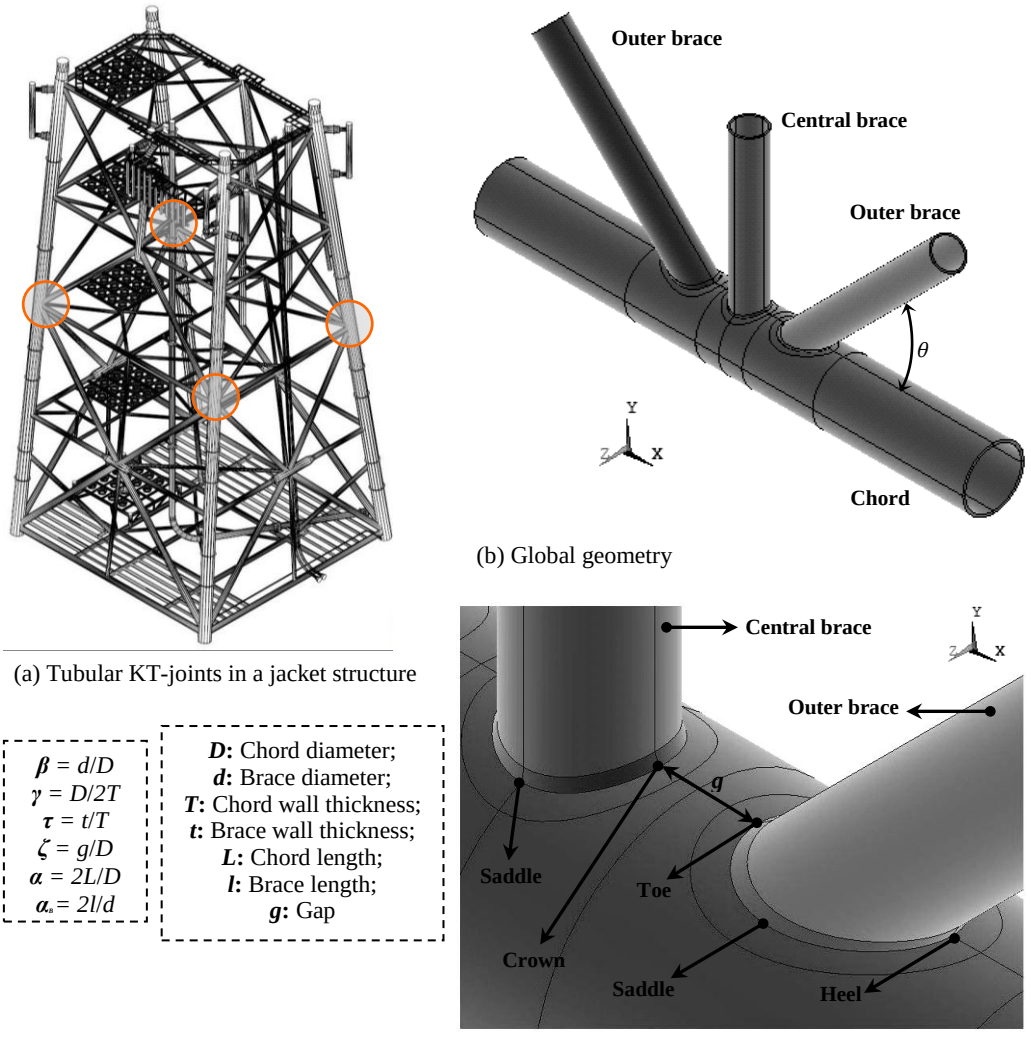

(a) Tubular KT-joints in a jacket structure

(b) Global geometry

(c) Critical positions along the weld toe

Figure1. Geometrical notation for a simple uniplanar KT-joint

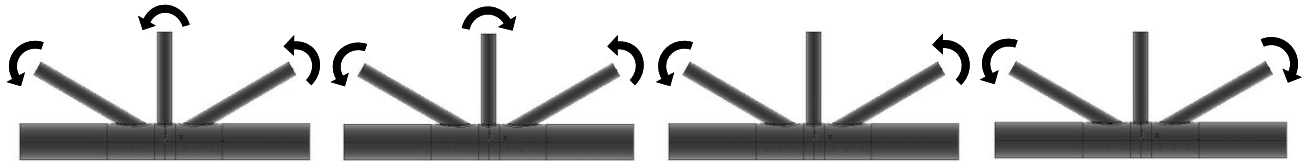

1st IPB loading condition | 2nd IPB loading condition | 3rd IPB loading condition | 4th IPB loading condition

Figure 2. Considered IPB loading conditions

2. FE modeling

2.1. Weld profile

One of the most critical factors affecting the accuracy of SCF results is accurate modeling of the weld profile. In the present research, the welding size along the brace/chord intersection satisfies the AWS D 1.1 [49] specifications. The dihedral angle (ψ) which is an important parameter in determining the weld thickness is defined as the angle between the chord and brace surface along the intersection curve. The dihedral angle at four typically important positions along the weld toe of central and outer braces can be determined as follows:

$$\psi = \begin{cases} \pi/2 & \text{Crown} \\ \pi - \cos^{-1}\theta & \text{Saddle} \\ \pi - \theta & \text{Toe} \\ \theta & \text{Heel} \end{cases} \quad (1)$$

where θ is the outer brace inclination angle (Figure 1b).

Details of weld profile modeling according to AWS D 1.1 [49] have been presented by Ahmadi et al. [28].

2.2. Boundary conditions

The chord end fixity conditions of tubular joints in offshore structures may range from almost fixed to almost pinned with generally being closer to almost fixed [5]. In practice, value of the parameter α in over 60% of tubular joints is in excess of 20 and is bigger than 40 in 35% of the joints [7]. Changing the end restraint from fixed to pinned results in a maximum increase of 15% in the SCF at crown position for α = 6 joints, and this increase reduces to only 8% for α = 8 [14]. In view of the fact that the effect of chord end restraints is only significant for joints with $\alpha < 8$ and high β and γ values, which do not commonly occur in practice, both chord ends were assumed to be fixed, with the corresponding nodes restrained.

Due to the XY-plane symmetry in the geometry and loading of the joint, only half of the entire KT-joint is required to be modeled. Appropriate symmetric boundary conditions were defined for the nodes located on the XY-plane crossing the centroid of the chord.

2.3. Mesh

In the present study, ANSYS element type SOLID95 was used to model the chord, braces, stiffeners, and the weld profiles. These elements have compatible displacements and are well-suited to model curved boundaries. The element is defined by 20 nodes having three degrees of freedom per node and may have any spatial orientation. Using this type of 3-D brick elements, the weld profile can be modeled as a sharp notch. This method will produce more accurate and detailed stress distribution near the intersection in comparison with a simple shell analysis.

In order to guarantee the mesh quality, a sub-zone mesh generation method was used during the FE modeling. In this method, the entire structure is divided into several different zones according to the computational requirements. The mesh of each zone is generated separately and then the mesh of entire structure is produced by merging the meshes of all the sub-zones. This method can easily control the mesh quantity and quality and avoid badly distorted elements. The mesh generated by this method for a uniplanar tubular KT-joint is shown in Figure 3.

As mentioned earlier, in order to determine the SCF, the stress at the weld toe should be divided by the nominal stress of the loaded brace. The stresses perpendicular to the weld toe at the extrapolation points are required to be calculated in order to determine the stress at the weld toe position. To extract and extrapolate the stresses perpendicular to the weld toe, as shown in Figure 3, the region between the weld toe and the second extrapolation point was meshed in such a way that each extrapolation point was placed between two nodes located in its immediate vicinity. These nodes are located on the element-generated paths which are perpendicular to the weld toe.

In order to verify the convergence of FE results, convergence test with different mesh densities was conducted before generating the 46 FE models for the parametric study.

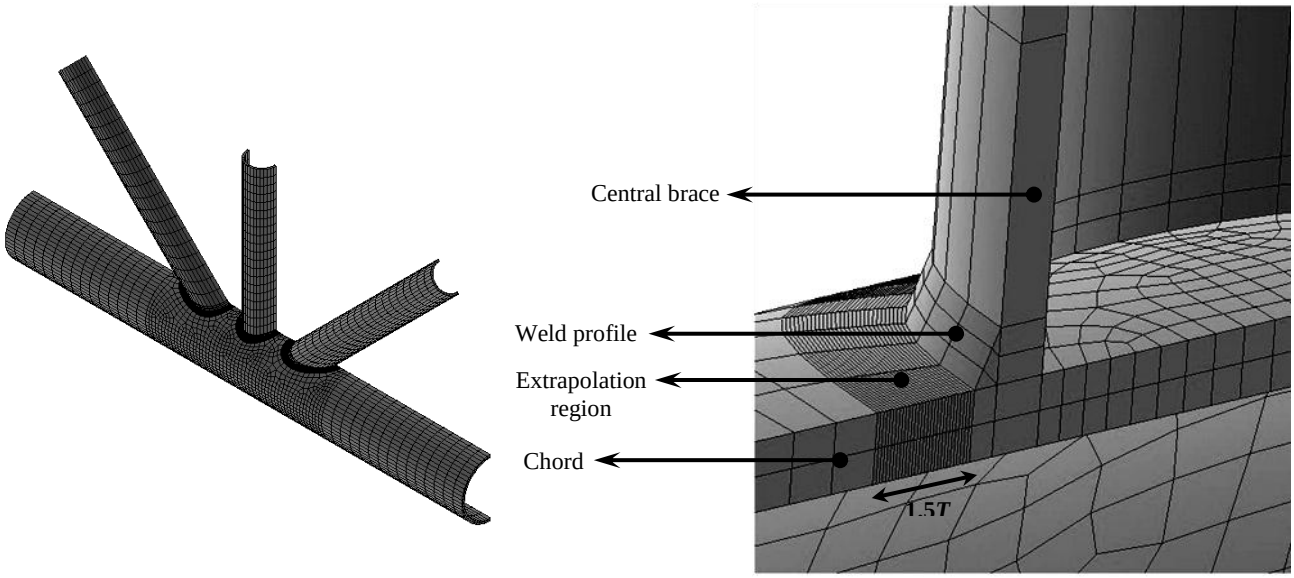

(a) Global view of the generated mesh

(b) Mesh generated in the regions adjacent to the intersection

Figure 3. Generated mesh in the regions adjacent to the brace/chord intersection: (a) Central brace, (b) Outer brace

2.4. Analysis and computation of SCFs

Static analysis of the linearly elastic type is suitable to determine the SCFs in tubular joints [50]. The Young's modulus and Poisson's ratio were taken to be 207 GPa and 0.3, respectively.

To determine the SCF, the stress at the weld toe position should be extracted from the stress field outside the region influenced by the local weld toe geometry. The location from which the stresses have to be extrapolated, *extrapolation region*, depends on the dimensions of the joint and on the position along the intersection. According to the linear extrapolation method recommended by IIW-XV-E [51], the first extrapolation point must be at a distance of 0.4T from the weld toe, and the second point should lie at 1.0T further from the first point (Figure 4a).

At an arbitrary node inside the extrapolation region, the stress component in the direction perpendicular to the weld toe can be calculated, through the transformation of primary stresses in the global coordinate system, using the following equation:

$$\sigma_{\perp N} = \sigma_x l_1^2 + \sigma_y m_1^2 + \sigma_z n_1^2 + 2\left(\tau_{xy} l_1 m_1 + \tau_{yz} m_1 n_1 + \tau_{zx} n_1 l_1\right) \quad (2)$$

where σ_a and τ_{ab} (a, b = x, y, z) are components of the stress tensor which can be extracted from ANSYS analysis results; and l_1, m_1, and n_1 are transformation components.

At the crown, toe, and heel positions, Eq. (2) is simplified as:

$$\sigma_{\perp N} = \sigma_x \quad (3)$$

The stress at an extrapolation point is obtained as follows:

$$\sigma_{\perp E} = \frac{\sigma_{\perp N1} - \sigma_{\perp N2}}{\delta_1 - \delta_2}\left(\Delta - \delta_2\right) + \sigma_{\perp N2} \quad (4)$$

where $\sigma_{\perp Ni}$ (i = 1 and 2) is the nodal stress in the immediate vicinity of the extrapolation point in a direction perpendicular to the weld toe (Eq. (3)); δ_i (i = 1 and 2) is the distance between the weld toe and the considered node inside the extrapolation region (Eq. (5)); and Δ equals to 0.4T and 1.4T for the first and second extrapolation points, respectively (Figure 4b).

The parameter δ is determined as follows:

$$\delta = \sqrt{\left(x_w - x_n\right)^2 + \left(y_w - y_n\right)^2 + \left(z_w - x_n\right)^2} \quad (5)$$

where (x_n , y_n , z_n) and (x_w , y_w , z_w) are global coordinates of the considered node inside the extrapolation region and its corresponding node at the weld toe position, respectively.

The extrapolated stress at the weld toe position which is perpendicular to the weld toe is calculated by the following equation:

$$\sigma_{\perp W} = 1.4\sigma_{\perp E1} - 0.4\sigma_{\perp E2} \quad (6)$$

where $\sigma_{\perp E1}$ and $\sigma_{\perp E2}$ are the stresses at the first and second extrapolation points in the direction perpendicular to the weld toe, respectively (Eq. (4)).

Finally, the SCF at the weld toe is obtained as:

$$\text{SCF} = \sigma_{\perp W} / \sigma_n \quad (7)$$

where σ_n is the nominal stress of the IPB-loaded brace which is calculated as follows:

$$\sigma_n = \frac{32 d M_i}{\pi\left[d^4 - \left(d - 2t\right)^4\right]} \quad (8)$$

where M_i is the in-plane bending moment.

To facilitate the SCF calculation, above formulation was implemented in a *macro* developed by the ANSYS Parametric Design Language (APDL). The input data required to be provided by the user of the macro are the node number at the weld toe, the chord

thickness, and the numbers of the nodes inside the extrapolation region. These nodes can be introduced using the Graphic user interface (GUI).

2.5. Verification of the FE results based on the experimental data

In order to validate the developed FE modeling procedure, a validation FE model was generated and its results were compared with the results of experimental tests carried out by Ahmadi et al. [39]. Details of test setup and program are not presented here for the sake of brevity.

The specimen fabricated by Ahmadi et al. [39] was tested under axial loading. In order to validate the FE models based on the data extracted from this experiment, the FE model of tested specimen was generated and analyzed under axial loading. The method of geometrical modeling (introducing the chord, braces, stiffeners, and weld profiles), the mesh generation procedure (including the selection of the element type and size), the analysis method, and the method of SCF extraction are identical for the validating model and the IPB-loaded joints used here for the parametric study. Hence, the verification of SCFs derived from axially-loaded FE model with corresponding experimental values lends some support to the validity of SCFs derived from IPB-loaded FE models. Moreover, in order to make sure that the IPB loading was correctly defined in ANSYS, nominal stresses obtained from the software were verified against the results of theoretical solid mechanics relations.

In Figure 5, experimental data and FE results have been compared. In this figure, the weld-toe SCF distribution along the central brace/chord intersection is presented. Due to the symmetry in the joint geometry and loading (XY- and YZ-plane symmetries), the SCF distribution along the weld toe of central brace is symmetric and only one fourth of the 360˚ brace/chord intersection, between the crown and saddle positions, is required to be considered. The polar angle (φ) along the 360˚ curve of the weld path is measured from the crown position. Hence, values of φ at the crown and saddle positions are 0˚ and 90˚, respectively. As can be seen in Figure 5, there is a good agreement between the test results and FE predictions. Hence, generated FE models can be considered to be accurate enough to provide valid results.

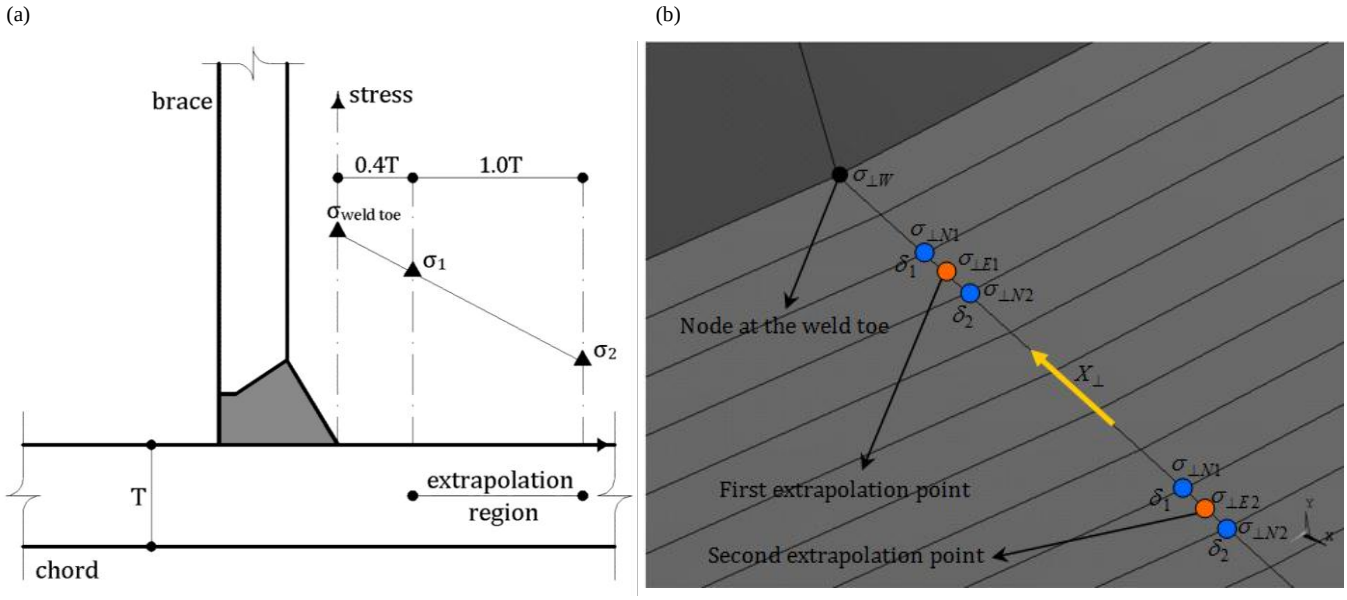

Figure 4. (a) Extrapolation procedure recommended by IIW-XV-E [51], (b) Required interpolations and extrapolations to extract SCFs based on the stresses perpendicular to the weld toe

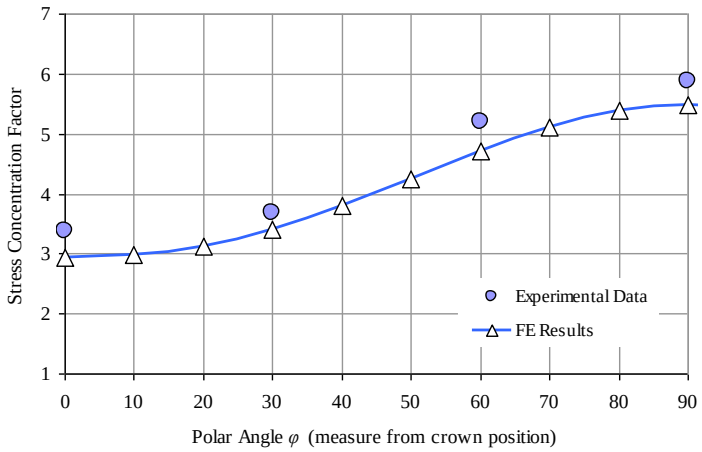

Figure 5. Distribution of chord-side SCFs along the central brace/chord intersection of uniplanar KT-joint: Comparison of the experimental data and FE results

3. Geometrical effects on the SCF values

3.1. Details of parametric study

In order to study the SCFs in uniplanar tubular KT-joints subjected to four types of IPB loading (Figure 2), 46 models were generated and analyzed using the FE software, ANSYS. The objective was to investigate the effects of non-dimensional geometrical parameters on the chord-side SCFs at the crown, toe, and heel position. As mentioned earlier, the saddle position was not studied. The reason is that under the IPB loadings, the nominal stress at this position is zero and hence the determination of SCFs is not needed.

Different values assigned for parameters β, γ, τ, and θ have been presented in Table 1. These values cover the practical ranges of the dimensionless parameters typically found in tubular joints of offshore jacket structures. Providing that the gap between the central and outer braces is not very large, the relative gap ($\zeta = g/D$) has no considerable effect on the SCF values in a tubular KT-joint. The validity range for this conclusion is $0.2 \le \zeta \le 0.6$ [20]. Hence, a typical value of $\zeta = 0.3$ was designated for all joints. Sufficiently long chord greater than six chord diameters (i.e. $\alpha \ge 12$) should be used to ensure that the stresses at the brace/chord intersection are not affected by the chord's boundary conditions [5]. Hence, in this study, a realistic value of $\alpha = 16$ was designated for all the models. The brace length has no effect on SCFs when the parameter α_B is greater than the critical value [16]. In the present study, in order to avoid the effect of short brace length, a realistic value of $\alpha_B = 8$ was assigned for all joints.

The 46 generated models span the following ranges of the geometric parameters:

$$0.4 \le \beta \le 0.6$$
$$12 \le \gamma \le 24$$
$$0.4 \le \tau \le 1.0 \quad (9)$$
$$30^\circ \le \theta \le 60^\circ$$

Table 1. Values assigned to each dimensionless parameter

Parameter	Definition	Values
β	d/D	0.4, 0.5, 0.6
γ	$D/2T$	12, 18, 24
τ	t/T	0.4, 0.7, 1.0
θ		30˚, 45˚, 60˚
ζ	g/D	0.3
α	$2L/D$	16
α_B	$2l/d$	8

3.2. Effect of the τ on the SCFs

The parameter τ is the ratio of brace thickness to chord thickness and the γ is the ratio of radius to thickness of the chord. Hence, the increase of the τ in models having constant value of the γ results in the increase of the brace thickness. This section presents the results of investigating the effect of the τ on the SCFs. In this study, the influence of parameters β, γ, and θ over the effect of the τ on SCFs was also investigated. For example, three charts are given in Figure 6 depicting the change of chord-side SCFs at the crown, toe, and heel positions, under the 1st loading condition, due to the change in the value of the τ and the interaction of this parameter with the θ. Altogether, 40 comparative charts were used to study the effect of the τ and only three of them are presented here for the sake of brevity.

Results showed that the increase of the τ leads to the increase of SCFs at the crown, toe, and heel positions under all studied IPB loading conditions. This result is not dependent on the values of other geometrical parameters. It was observed that the SCFs at the crown position of the central brace are bigger that the corresponding values at the toe and heel positions of the outer brace. It can also be concluded that at the crown and heel positions, the effect of changing the parameter τ on the SCF values is greater than the effect of the parameter θ.

3.3. Effect of the β on the SCFs

The parameter β is the ratio of brace diameter to chord diameter. Hence, the increase of the β in models having constant value of chord diameter results in the increase of brace diameter. This section presents the results of investigating the effect of the β on the SCFs. In this study, the interaction of the β with the other geometrical parameters was also investigated. Figure 7 demonstrates the change of SCFs at the crown, toe, and heel positions, under the 1st loading condition, due to the change in the value of the β and the interaction of this parameter with the γ.

Through investigating the effect of the β on the SCFs, it can be concluded that the increase of the β does not have a considerable effect on the SCF values at the crown, toe, and heel positions. This conclusion is not dependent on either the type of applied IPB load or the values of other geometrical parameters. It is also evident that, in spite of the parameter β, the parameter γ is quite effective in increasing the SCF values.

3.4. Effect of the γ on the SCFs

The parameter γ is the ratio of radius to thickness of the chord. Hence, the increase of the γ in models having constant value of the chord diameter means the decrease of chord thickness. This section presents the results of investigating the effect of the γ on the SCFs. In this study, the influence of parameters β, τ, and θ over the effect of the γ on SCFs was also investigated. For example, three charts are presented in Figure 8 depicting the change of SCFs, at the crown, toe, and heel positions, due to the change in the value of the γ and the interaction of this parameter with the τ, under the 1st loading condition. Altogether, 40 comparative charts were used to study the effect of the γ and only three of them are presented here for the sake of brevity.

It was observed that under all considered IPB loading conditions, the increase of the γ results in the increase of SCFs at the crown, toe, and heel positions.

3.5. Effect of the θ on the SCFs

This section presents the results of studying the effect of the outer brace inclination angle θ on SCFs and its interaction with the other geometrical parameters. Three charts are given in Figure 9, as an example, depicting the change of SCFs at the crown, toe, and heel positions, under the 1st loading condition, due to the change in the value of θ and the interaction of this parameter with the β.

Through investigating the effect of the θ on the SCF values, it can be concluded that the increase of the θ leads to the increase of SCFs at all three considered positions. However, the amount of SCF change at the crown position is not considerable. Also, the increase of SCF at the toe position is more than its increase at the heel position.

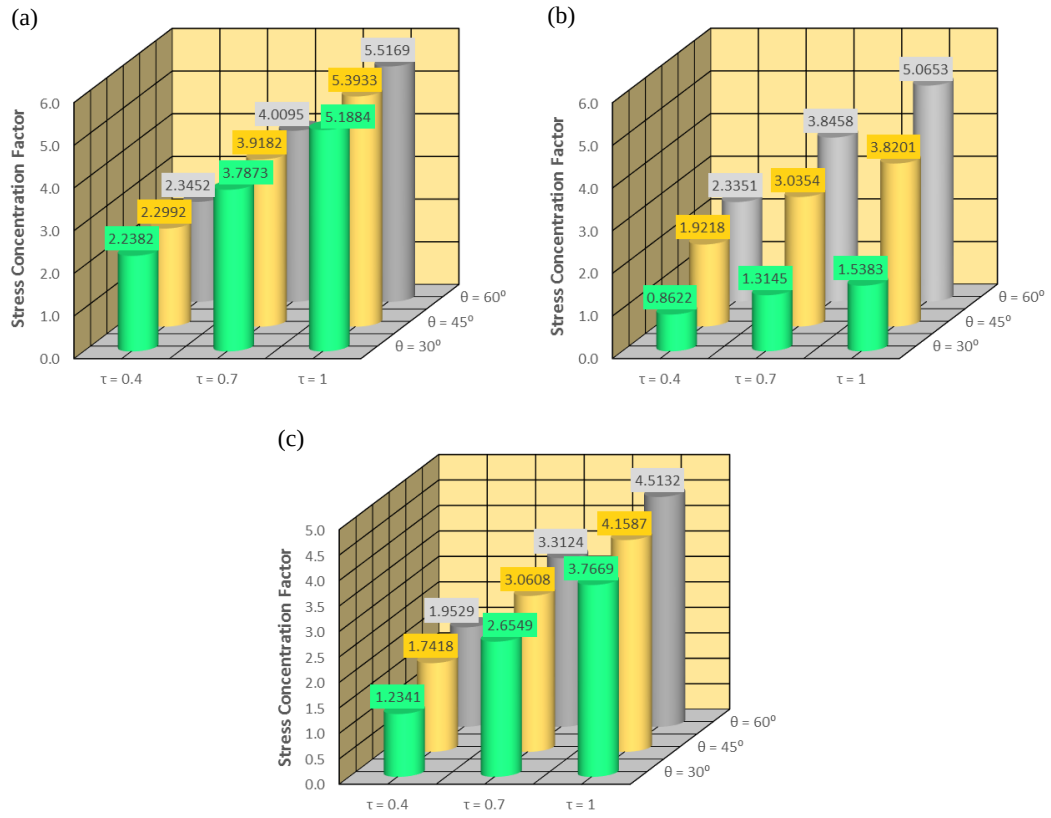

Figure 6. Effect of the τ on the SCFs under the 1st IPB loading condition (β = 0.6, γ = 24): (a) Crown position, (b) Toe position, (c) Heel position

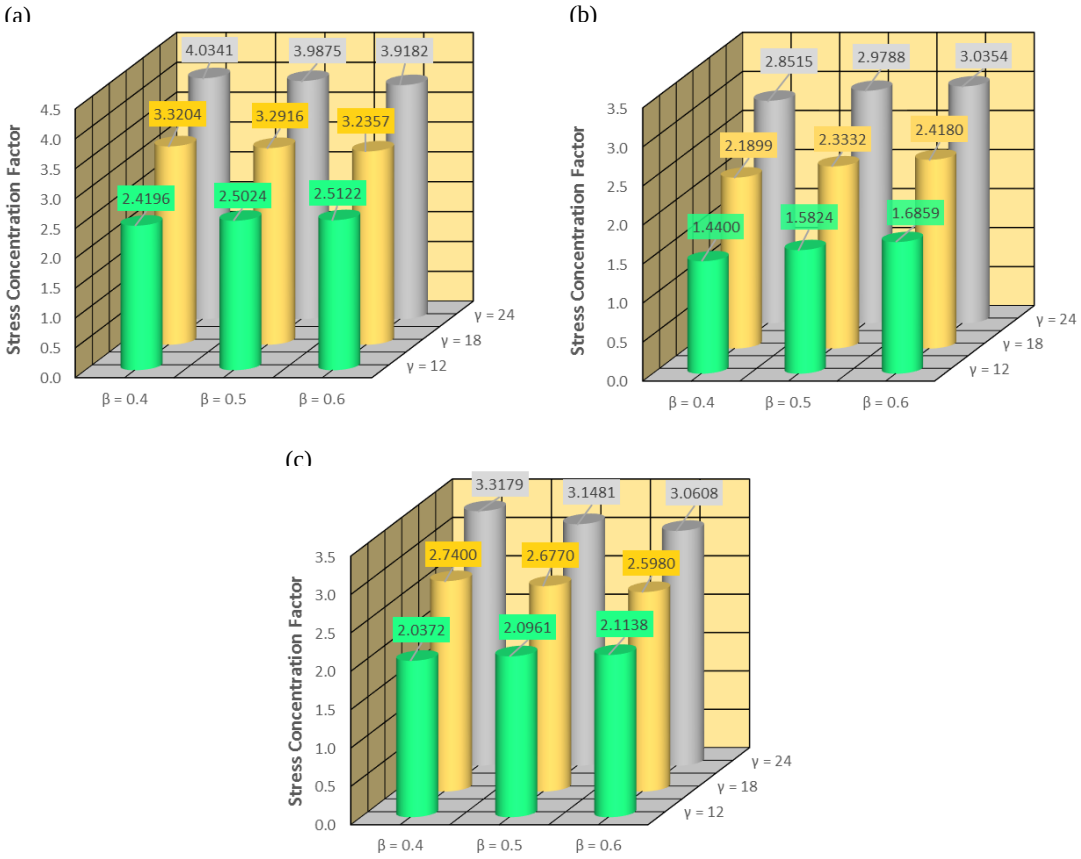

Figure 7. Effect of the β on the SCFs under the 1st IPB loading condition ($\theta = 45^{\circ}$, $\tau = 0.7$): (a) Crown position, (b) Toe position, (c) Heel position

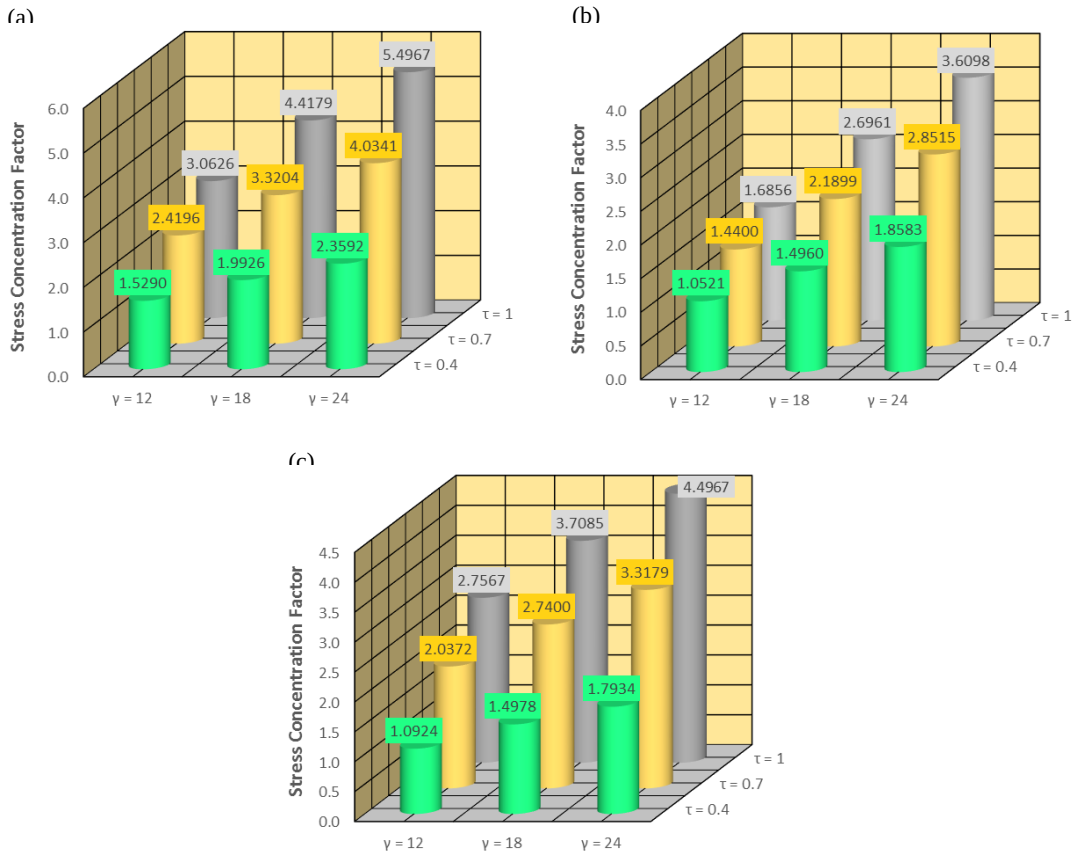

Figure 8. Effect of the γ on the SCFs under the 1st IPB loading condition ($\theta = 45^{\circ}$, $\beta = 0.4$): (a) Crown position, (b) Toe position, (c) Heel position

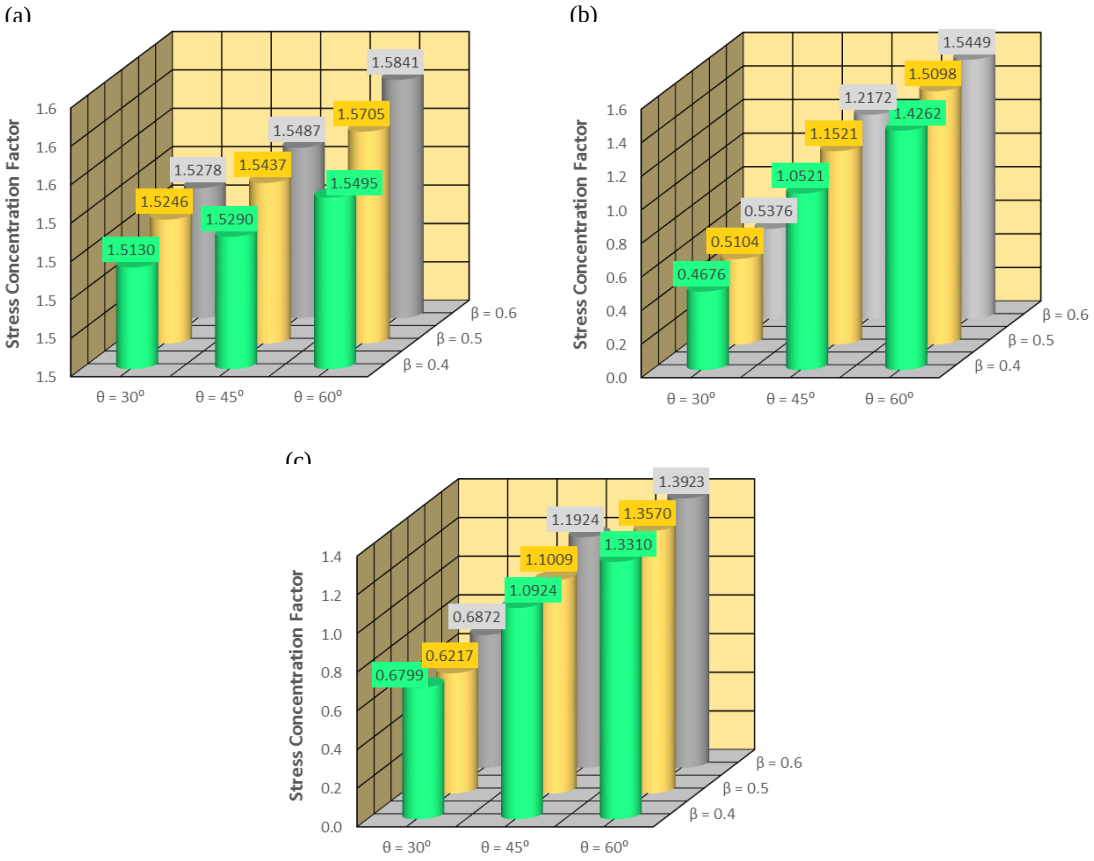

Figure 9. Effect of the θ on the SCFs under the 1st IPB loading condition (τ = 0.4, γ = 12): (a) Crown position, (b) Toe position, (c) Heel position

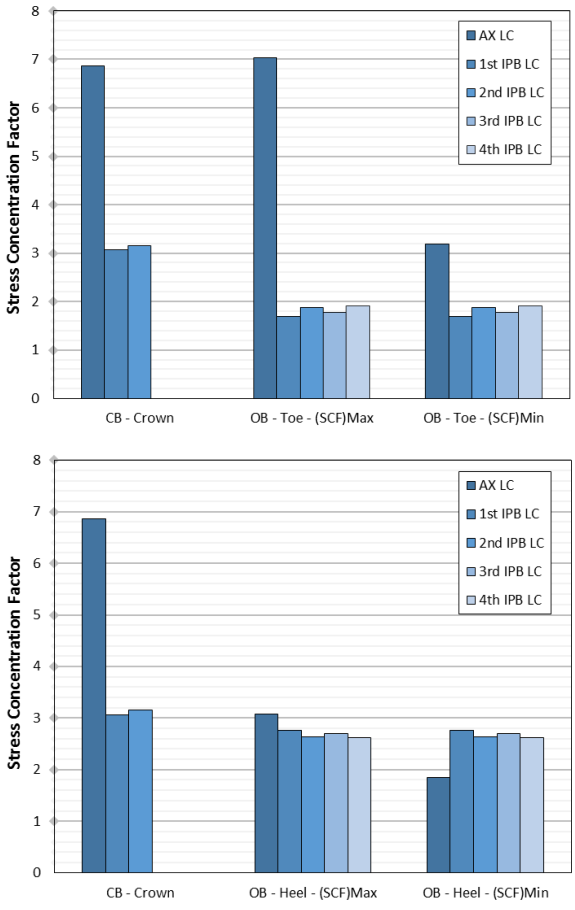

Figure 10. Comparison of chord-side SCFs under axial and IPB loading conditions (θ = 45°, β = 0.4, τ = 1.0, γ = 12)

3.6. Comparison of SCFs at different positions and under different loading conditions

In Figure 10, the SCFs extracted from tubular joints subjected to axial and IPB loadings have been compared at different positions. SCFs of the axially loaded joints are cited from Ahmadi et al. [38, 39]. It is evident that, at all three considered positions, i.e. crown, toe, and heel, the maximum SCFs under the axial loading are much bigger than the corresponding values under IPB loading conditions. This conclusion implies that if the SCF design equations developed for the axially-loaded KT-joints are used for the SCF calculation in the IPB-loaded joints, result will be unrealistic and highly conservative. Hence, it is necessary to establish SCF formulas for IPB-loaded joints of this type. Figure 10 also indicated that the SCF at the crown position is higher than the corresponding values at the toe and heel positions.

By comparing the SCFs under four considered IPB loadings, according to Figure 10, it can be concluded that:

Crown:

$$SCF_{2nd\ IPB\ LC} > SCF_{1st\ IPB\ LC} \quad (10)$$

Toe:

$$SCF_{4th\ IPB\ LC} > SCF_{2nd\ IPB\ LC} > SCF_{3rd\ IPB\ LC} > SCF_{1st\ IPB\ LC} \quad (11)$$

Heel:

$$SCF_{1st\ IPB\ LC} > SCF_{3rd\ IPB\ LC} > SCF_{2nd\ IPB\ LC} > SCF_{4th\ IPB\ LC} \quad (12)$$

where LC stands for loading condition.

4. Deriving parametric equations for the SCF calculation

In the present paper, 10 individual parametric equations are proposed to determine the chord-side SCFs at the crown, toe, and heel positions on the weld toe of central and outer braces in simple uniplanar tubular KT-joints subjected to four types of IPB loading. For all considered IPB load cases, results indicated that at the central brace, the maximum value of the SCF along the weld toe always occurs at the crown position; and at the outer brace, the maximum value of the weld-toe SCF always occurs at either the toe or the heel positions. Hence, proposed equations cover all of the critical positions.

Parametric SCF design equations were derived based on multiple nonlinear regression analyses performed by the statistical software package, SPSS. Values of dependent variable (i.e. SCF) and independent variables (i.e. β, γ, τ, and θ) constitute the input data imported in the form of a matrix. Each row of this matrix involves the information about the SCF value at the considered position on the weld toe of central/outer brace in a uniplanar tubular KT-joint having specific geometrical characteristics.

When the dependent and independent variables are defined, a model expression must be built with defined parameters. Parameters of the model expression are unknown coefficients and exponents. The researcher must specify a starting value for each parameter, preferably as close as possible to the expected final solution. Poor starting values can result in failure to converge or in convergence on a solution that is local (rather than global) or is physically impossible. Various model expressions must be built to derive a parametric equation having a high coefficient of determination (R^2).

After performing a large number of nonlinear analyses, following parametric equations are proposed for the calculation of chord-side SCFs at the crown, toe, and heel positions on the weld toe of central and outer braces in simple uniplanar tubular KT-joints subjected to four types of IPB loads (Figure 2):

- **Central brace, Crown position:**

1st loading condition:

$$SCF = 0.566\ \tau^{0.883}\gamma^{0.715}\beta^{-0.003}\theta^{0.061}$$
$$R^2 = 0.994 \quad (13)$$

2nd loading condition:

$$SCF = 0.671\ \tau^{0.848}\gamma^{0.683}\beta^{0.115}\theta^{0.023}$$
$$R^2 = 0.976 \quad (14)$$

- **Outer brace, Toe position:**

1st loading condition:

$$SCF = 0.332\ \tau^{0.734}\gamma^{0.868}\beta^{0.131}\theta^{1.487}$$
$$R^2 = 0.968 \quad (15)$$

2nd loading condition:

$$SCF = 0.495\ \tau^{0.743}\gamma^{0.755}\beta^{0.270}\theta^{0.902}$$
$$R^2 = 0.969 \quad (16)$$

3rd loading condition:

$$SCF = 0.411\ \tau^{0.744}\gamma^{0.798}\beta^{0.164}\theta^{1.193}$$
$$R^2 = 0.981 \quad (17)$$

4th loading condition:

$$SCF = 0.454\ \tau^{0.754}\gamma^{0.791}\beta^{0.219}\theta^{1.064}$$
$$R^2 = 0.981 \quad (18)$$

- **Outer brace, Heel position:**

1st loading condition:

$$SCF = 0.631\ \tau^{0.993}\gamma^{0.623}\beta^{-0.061}\theta^{0.384}$$
$$R^2 = 0.984 \quad (19)$$

2nd loading condition:

$$SCF = 0.455\ \tau^{1.025}\gamma^{0.727}\beta^{-1.01}\theta^{0.590}$$
$$R^2 = 0.975 \quad (20)$$

3rd loading condition:

$$SCF = 0.572\ \tau^{1.033}\gamma^{0.635}\beta^{-0.144}\theta^{0.470}$$
$$R^2 = 0.972 \quad (21)$$

4th loading condition:

$$SCF = 0.541\ \tau^{1.018}\gamma^{0.658}\beta^{-0.113}\theta^{0.523}$$
$$R^2 = 0.983 \quad (22)$$

In Eqs. (13)–(22), the parameter θ should be inserted in radians. Obtained values of R^2 are considered to be acceptable regarding the complex nature of the

problem. The validity ranges of non-dimensional geometrical parameters for the developed equations have been given in Eq. (9).

The UK DoE [48] recommends the following assessment criteria regarding the applicability of the commonly used SCF parametric equations (P/R stands for the ratio of the *predicted* SCF from a given equation to the *recorded* SCF from test or analysis):

- For a given dataset, if % SCFs under-predicting $\leq$ 25%, i.e. [%P/R < 1.0] $\leq$ 25%, and if % SCFs considerably under-predicting $\leq$ 5%, i.e. [%P/R < 0.8] $\leq$ 5%, then accept the equation. If, in addition, the percentage SCFs considerably over-predicting $\leq$ 50%, i.e. [%P/R > 1.5] $\geq$50%, then the equation is regarded as generally conservative.
- If the acceptance criteria is nearly met i.e. 25% < [%P/R < 1.0] $\leq$ 30%, and/or 5% < [%P/R < 0.8] $\leq$ 7.5%, then the equation is regarded as borderline and engineering judgment must be used to determine acceptance or rejection.
- Otherwise reject the equation as it is too optimistic.

In view of the fact that for a mean fit equation, there is always a large percentage of under-prediction, the requirement for joint under-prediction, i.e. P/R < 1.0, can be completely removed in the assessment of parametric equations [52]. Assessment results according to the UK DoE [48] criteria are presented in Table 2.

As can be seen in Table 2, all of the proposed equations satisfy the UK DoE criteria; and hence, they can reliably be used for the fatigue design of offshore jacket structures.

Table 2. Assessment of developed equations based on the UK DoE [48] criteria

Brace	Position	Loading Condition	Equation	UK DoE Conditions		Decision
				%P/R < 0.8	%P/R > 1.5	
Central	Crown	1st	Eq. (13)	0% < 5% OK.	0% < 50% OK.	Accept
Central	Crown	2nd	Eq. (14)	0% < 5% OK.	0% < 50% OK.	Accept
Outer	Toe	1st	Eq. (15)	2.7% < 5% OK.	5.5% < 50% OK.	Accept
Outer	Toe	2nd	Eq. (16)	0% < 5% OK.	2.7% < 50% OK.	Accept
Outer	Toe	3rd	Eq. (17)	0% < 5% OK.	0% < 50% OK.	Accept
Outer	Toe	4th	Eq. (18)	0% < 5% OK.	0% < 50% OK.	Accept
Outer	Heel	1st	Eq. (19)	0% < 5% OK.	0% < 50% OK.	Accept
Outer	Heel	2nd	Eq. (20)	0% < 5% OK.	2.7% < 50% OK.	Accept
Outer	Heel	3rd	Eq. (21)	0% < 5% OK.	0% < 50% OK.	Accept
Outer	Heel	4th	Eq. (22)	0% < 5% OK.	5.5% < 50% OK.	Accept

5. Conclusions

Results of stress analysis performed on 46 FE models verified using experimental data were used to investigate the effect of geometrical parameters on the chord-side SCFs at the crown, toe, and heel positions along the weld toe of central and outer braces in simple uniplanar tubular KT-joints under four types of IPB loading. A set of SCF parametric equations was also developed for the fatigue design. Main conclusions are summarized as follows:

- The SCFs at the crown position of the central brace are bigger that the corresponding values at the toe and heel positions of the outer brace.
- The increase of the parameters τ and/or γ leads to the increase of SCFs at the crown, toe, and heel positions.
- The increase of the β does not have a considerable effect on the SCF values at the considered positions.
- The increase of the θ leads to the increase of SCFs at all three considered positions. However, the amount of SCF change at the crown position is not considerable. Also, the increase of SCF at the toe position is more than its increase at the heel position.
- At the crown and heel positions, the effect of changing the parameter τ on the SCF values is greater than the effect of the parameter θ. These conclusions are valid for all considered IPB loadings.
- At all of three considered positions, the SCFs under the axial loading are much bigger than the corresponding values under IPB loading conditions. This conclusion implies that if the SCF parametric equations developed for axially-loaded KT-joints are used for the SCF calculation in the IPB-loaded joints, result will be unrealistic and highly conservative. Consequently, it is important to derive SCF parametric formulas specifically for IPB-loaded joints of this type.
- Relatively high coefficients of determination and the satisfaction of acceptance criteria recommended by the UK DoE guarantee the accuracy of 10 parametric equations derived in the present paper. Hence, the proposed equations can reliably be used for the fatigue analysis and design of uniplanar tubular KT-joints.

Acknowledgements

The authors would like to thank Mr. Esmaeil Zavvar for his help during the numerical study. Anonymous

reviewers are also gratefully acknowledged for their useful comments on draft version of this paper.

References

1- Kuang, J.G., Potvin, A.B. and Leick, R.D., (1975), *Stress concentration in tubular joints*, Proceedings of the Offshore Technology Conference, Paper OTC 2205, Houston (TX), US.

2- Wordsworth, A.C. and Smedley, G.P., (1978), *Stress concentrations at unstiffened tubular joints*, Proceedings of the European Offshore Steels Research Seminar, Paper 31, Cambridge, UK.

3- Wordsworth, A.C., (1981), *Stress concentration factors at K and KT tubular joint*, Proceedings of the Conference on Fatigue of Offshore Structural Steels, p. 59-69.

4- Efthymiou, M. and Durkin, S., (1985), *Stress concentrations in T/Y and gap/overlap K-joints*, Proceedings of the Conference on Behavior of Offshore Structures, Delft, the Netherlands, p. 429-440.

5- Efthymiou, M., (1988), *Development of SCF formulae and generalized influence functions for use in fatigue analysis*, OTJ 88, Surrey, UK.

6- Hellier, A.K., Connolly, M. and Dover, W.D., (1990), *Stress concentration factors for tubular Y and T-joints*. International Journal of Fatigue, Vol. 12, p. 13-23.

7- Smedley, P. and Fisher, P., (1991), *Stress concentration factors for simple tubular joints*, Proceedings of the International Offshore and Polar Engineering Conference (ISOPE), Edinburgh, p. 475-483.

8- UK Health and Safety Executive, (1997), *OTH 354: stress concentration factors for simple tubular joints-assessment of existing and development of new parametric formulae*, Prepared by Lloyd's Register of Shipping, UK.

9- Karamanos, S.A., Romeijn, A., Wardenier, J., (2000), *Stress concentrations in tubular gap K-joints: mechanics and fatigue design*, Engineering Structures, Vol. 22, p. 4-14.

10- Gho, W.M. and Gao, F., (2004), *Parametric equations for stress concentration factors in completely overlapped tubular K(N)-joints*, Journal of Constructional Steel Research, Vol. 60, p. 1761-1782.

11- Gao, F., (2006), *Stress and strain concentrations of completely overlapped tubular joints under lap brace OPB load*. Thin-Walled Structures, Vol. 44, p. 861-871.

12- Gao, F., Shao, Y.B. and Gho, W.M., (2007), *Stress and strain concentration factors of completely overlapped tubular joints under lap brace IPB load*. Journal of Constructional Steel Research, Vol. 63, p. 305-316.

13- Morgan, M.R. and Lee, M.M.K., (1998), *Parametric equations for distributions of stress concentration factors in tubular K-joints under out-of-plane moment loading*, International Journal of Fatigue, Vol. 20, p. 449-461.

14- Morgan, M.R. and Lee, M.M.K., (1998), *Prediction of stress concentrations and degrees of bending in axially loaded tubular K-joints*, Journal of Constructional Steel Research, Vol. 45, pp. 67-97.

15- Chang, E. and Dover, W.D., (1999), *Prediction of stress distributions along the intersection of tubular Y and T-joints*, International Journal of Fatigue, Vol. 21, p. 361-381.

16- Chang, E. and Dover, W.D., (1999), *Parametric equations to predict stress distributions along the intersection of tubular X and DT-joints*, International Journal of Fatigue, Vol. 21, p. 619-635.

17- Shao, Y.B., (2004), *Proposed equations of stress concentration factor (SCF) for gap tubular K-joints subjected to bending load*, International Journal of Space Structures, Vol. 19, 137-147.

18- Shao, Y.B., (2007), *Geometrical effect on the stress distribution along weld toe for tubular T- and K-joints under axial loading*, Journal of Constructional Steel Research, Vol. 63, p. 1351-1360.

19- Shao, Y.B., Du, Z.F. and Lie, S.T., (2009), *Prediction of hot spot stress distribution for tubular K-joints under basic loadings*, Journal of Constructional Steel Research, Vol. 65, p. 2011-2026.

20- Lotfollahi-Yaghin, M.A. and Ahmadi, H., (2010), *Effect of geometrical parameters on SCF distribution along the weld toe of tubular KT-joints under balanced axial loads*, International Journal of Fatigue, Vol. 32, p. 703-719.

21- Ahmadi, H., Lotfollahi-Yaghin, M.A. and Aminfar, M.H., (2011), *Geometrical effect on SCF distribution in uni-planar tubular DKT-joints under axial loads*, Journal of Constructional Steel Research, Vol. 67, 1282-1291.

22- Karamanos, S.A. Romeijn, A. and Wardenier, J., (1999), *Stress concentrations in multi-planar welded CHS XX-connections*, Journal of Constructional Steel Research, Vol. 50, p. 259-282.

23- Chiew, S.P., Soh, C.K. and Wu, N.W., (2000), *General SCF design equations for steel multiplanar tubular XX-joints*, International Journal of Fatigue, Vol. 22, p. 283-293.

24- Wingerde, A.M., Packer, J.A. and Wardenier, J., (2001), *Simplified SCF formulae and graphs for CHS and RHS K- and KK-connections*. Journal of Constructional Steel Research, Vol. 57, 221-252.

25- Karamanos, S.A., Romeijn, A. and Wardenier, J., (2002), *SCF equations in multi-planar welded tubular DT-joints including bending effects*, Marine Structures, Vol. 15, p. 157-173.

26- Lotfollahi-Yaghin, M.A. and Ahmadi, H., (2011), *Geometric stress distribution along the weld toe of the outer brace in two-planar tubular DKT-joints: parametric study and deriving the SCF design equations*, Marine Structures, Vol. 24, p. 239-260.

27- Ahmadi, H., Lotfollahi-Yaghin, M.A. and Aminfar, M.H., (2011), *Distribution of weld toe stress concentration factors on the central brace in two-planar CHS DKT-connections of steel offshore structures*, Thin-Walled Structures, Vol. 49, p. 1225-1236.

28- Ahmadi, H., Lotfollahi-Yaghin, M.A. and Aminfar, M.H., (2012), *The development of fatigue design formulas for the outer brace SCFs in offshore three-planar tubular KT-joints*, Thin-Walled Structures, Vol. 58, p. 67-78.

29- Ahmadi, H., Lotfollahi-Yaghin, M.A., (2012), *Geometrically parametric study of central brace SCFs in offshore three-planar tubular KT-joints*, Journal of Constructional Steel Research, Vol. 71, p. 149-161.
30- Dharmavasan, S. and Aaghaakouchak, A.A., (1988), *Stress concentrations in tubular joints stiffened by internal ring stiffeners*, Proceedings of the Seventh International Conference on Offshore Mechanics and Arctic Engineering, Houston (TX), US, p. 141-148.
31- Aaghaakouchak, A.A. and Dharmavasan, S., (1990), *Stress analysis of unstiffened and stiffened tubular joints using improved finite element model of intersection*, Proceedings of the Ninth International Conference on Offshore Mechanics and Arctic Engineering, Vol. III, Part A, Houston (TX), US, p. 321-328.
32- Ramachandra Murthy, D.S., Madhava Rao, A.G., Ghandi, P. and Pant, P.K. (1992), *Structural efficiency of internally ring stiffened steel tubular joints*, Journal of Structural Engineering, Vol. 118, 3016-3035.
33- Nwosu, D.I., Swamidas, A.S.J. and Munaswamy, K., (1995), *Numerical stress analysis of internal ring-stiffened tubular T-joints*, Journal of Offshore Mechanics and Arctic Engineering, Vol. 117, p. 113-125.
34- Ramachandra, D.S., Gandhi, P., Raghava, G. and Madhava Rao, A.G., (2000), *Fatigue crack growth in stiffened steel tubular joints in seawater environment*, Engineering Structures, Vol. 22, p. 1390-1401.
35- Hoon, K.H., Wong, L.K. and Soh, A.K. (2001), *Experimental investigation of a doubler-plate reinforced tubular T-joint subjected to combined loadings*, Journal of Constructional Steel Research, Vol. 57, p. 1015-1039.
36- Myers, P.T., Brennan, F.P. and Dover, W.D., (2001), *The effect of rack/rib plate on the stress concentration factors in jack-up chords*, Marine Structures, Vol. 14, p. 485-505.
37- Woghiren, C.O. and Brennan, F.P., (2009), *Weld toe stress concentrations in multi planar stiffened tubular KK Joints*, International Journal of Fatigue, Vol. 31, p. 164-172.
38- Ahmadi, H., Lotfollahi-Yaghin, M.A., Shao, Y.B. and Aminfar, M.H., (2012), *Parametric study and formulation of outer-brace geometric stress concentration factors in internally ring-stiffened tubular KT-joints of offshore structures*, Applied Ocean Research, Vol. 38, p. 74-91.
39- Ahmadi, H., Lotfollahi-Yaghin, M.A. and Shao, Y.B., (2013), *Chord-side SCF distribution of central brace in internally ring-stiffened tubular KT-joints: A geometrically parametric study*, Thin-Walled Structures, Vol. 70, 93-105.
40- Ahmadi, H. and Lotfollahi-Yaghin, M.A., (2015), *Stress concentration due to in-plane bending (IPB) loads in ring-stiffened tubular KT-joints of offshore structures: Parametric study and design formulation*, Applied Ocean Research, Vol. 51, p. 54-66.
41- Ahmadi, H. and Zavvar, E., (2015), *Stress concentration factors induced by out-of-plane bending loads in ring-stiffened tubular KT-joints of jacket structures*, Thin-Walled Structures, Vol. 91, p. 82-95.
42- Ahmadi, H., Lotfollahi-Yaghin, M.A. and Aminfar, M.H., (2011), *Effect of stress concentration factors on the structural integrity assessment of multi-planar offshore tubular DKT-joints based on the fracture mechanics fatigue reliability approach*, Ocean Engineering, Vol. 38, p. 1883-1893.
43- Ahmadi, H. and Lotfollahi-Yaghin, M.A., (2012), *A probability distribution model for stress concentration factors in multi-planar tubular DKT-joints of steel offshore structures*, Applied Ocean Research, Vol. 34, 21-32.
44- Ahmadi, H. and Lotfollahi-Yaghin, M.A., (2013), *Effect of SCFs on S–N based fatigue reliability of multi-planar tubular DKT-joints of offshore jacket-type structures*, Ships and Offshore Structures, Vol. 8, p. 55-72.
45- Dallyn, P., El-Hamalawi, A., Palmeri, A. and Knight, R., (2015), *Experimental testing of grouted connections for offshore substructures: A critical review*, Structures, Vol. 3, p. 90-108.
46- Ahmadi, H., Mohammadi, A.H. and Yeganeh, A., (2015), *Probability density functions of SCFs in internally ring-stiffened tubular KT-joints of offshore structures subjected to axial load*, Thin-Walled Structures, 2015, Vol. 94, p. 485-499.
47- Ahmadi, H., Mohammadi, A.H., Yeganeh, A. and Zavvar, E., (2016), *Probabilistic analysis of stress concentration factors in tubular KT-joints reinforced with internal ring stiffeners under in-plane bending loads*, Thin-Walled Structures, Vol. 99, p. 58-75.
48- UK Department of Energy, (1983), *Background notes to the fatigue guidance of offshore tubular joints*, London, UK.
49- American Welding Society (AWS), (2002), *Structural welding code: AWS D 1.1*, Miami (FL), US.
50- N'Diaye, A., Hariri, S., Pluvinage, G. and Azari, Z., (2007), *Stress concentration factor analysis for notched welded tubular T-joints*, International Journal of Fatigue, Vol. 29, p. 1554-1570.
51- IIW-XV-E, (1999), *Recommended fatigue design procedure for welded hollow section joints, IIW Docs, XV-1035-99/XIII-1804-99*, International Institute of Welding, France.
52- Bomel Consulting Engineers, (1994), *Assessment of SCF equations using Shell/KSEPL finite element data*, C5970R02.01 REV C.